Low-Cost PWM Drive for an Electric Mini-Baja Type Vehicle

Samuel E. de Lucena
UNESP - São Paulo State University, Guaratinguetá, Brazil
lucena@feg.unesp.br

Francisco Jose Grandinetti
UNITAU - University of Taubaté, Taubaté, SP, Brazil
grandi@unitau.br

Marcio Abud Marcelino
UNESP - São Paulo State University, Guaratinguetá, SP, Brazil
abud@feg.unesp.br

Abstract— *This paperwork presents a Pulse Width Modulation (PWM) drive for an electric mini-baja-type car. The electric vehicle traction is provided by a battery-fed 1-kW three-phase induction motor. The open-loop speed control is implemented with an equal voltage/frequency ratio, in order to maintain a constant amount of torque on all velocities. The PWM is implemented by a low-cost 8-bit microcontroller provided with optimized ROM charts for distinct speed value implementations, synchronized transition between different charts and reduced odd harmonics generation. This technique was implemented using a single passenger mini-baja vehicle, and the essays have shown that its application resulted on reduced current consumption, besides eliminating mechanical parts.*

Keywords*: induction motor, electric vehicle, speed drive, PWM, microcontroller*

1. Introduction

The main purpose for using electric vehicles (EVs), as opposed to internal-combustion cars, is that they are zero-emission vehicles. Besides not giving off carbon dioxide to the atmosphere, which is one of the main causes for air pollution in metropolitan areas, EVs require virtually zero-maintenance, no periodic oil changes, mufflers that rust out, burst hoses, and so on, besides being tremendously silent. Motor and control technology for EVs are available today. The main problem found on vehicles supported by batteries is (battery) cost and, to some extent, the smaller range and the relatively time-consuming refueling, as compared to gasoline-powered cars. Fortunately, battery technology and costs are improving rapidly, and advanced nickel-hydride batteries are getting into volume production (Riezenman, 1998; Cocconi and Gage, 2002; Cooper, 2005; Lam et all, 2005).

Initially, main EVs producers decided to produce an EV with characteristics closest to gasoline-powered internal-combustion engines (ICEs), crossing distances of up to 240 km away with no battery re-charge and achieving speeds as high as 192 km/h. However, given that 40% of vehicles in megacities drive less than 60 km a day, an EV with a range of 150 km should be actually much attractive (Riezenman, 1998; Naunim, 1996; Main, 2005; Faiz, 2005).

As of now, there is not a consensus among automakers in regards to what motor, transmission, battery, and speed controller to use in EVs, creating many different combinations found on EVs in the marketplace today (Scaduto and Fenton, 1993). As environmentalists, government and automakers continue their struggle to make consumers confident in EVs, the following concepts on EV must be highlighted, if mankind is to breath clean air in megacities, and slow down planet warming:

1) The EV must be a small vehicle, providing transportation for four passengers at most. It cannot be the family's only car, but it should be the daily drive one, inasmuch as a huge amount of families have two or three cars. It should be used for distances of 200 km at the most. Therefore, it is an extremely attractive vehicle for going to work.

2) ICEs cannot be compared to EVs, for the reasons given above. Although EVs can accelerate as fast as ICEs, that would put the battery autonomy in jeopardy. EVs must have optimized acceleration slopes, which must be somewhat independent of the driver's need for acceleration. As a result, automakers cannot use traditional marketing concepts with potential buyers, if EVs are to be mass-produced and marketed worldwide.

Shortly, the EV must be lightweight, with the least number of moving parts, and with a limited number of electrical accessories (in tropical countries at least). This paperwork aims the study and implementation of an experimental EV, and emphasizes the use of a low-cost PWM drive.

2. Main Vehicle Features

The Mini-Baja is an ideal vehicle for sportive contests and educative goals. It is somewhat rugged and able to drive on almost any soil condition. It features rear wheel drive, which is powered by a four-cycle, eight horsepower, gasoline, air-cooled engine produced by Briggs & Stratton Corporation. It can achieve a top speed of 60 km/h. The one-passenger-seat car is made of tubular 1020 steel, and it is approximately 2.0 m x 1.0 m x 1.55 m, a between axle distance of 1.70 m, and a 205 kg mass, including five liters of gasoline in the fuel tank. It also features a conical

transmission with two stages of reduction by chains, with no reverse gear. There were not many mechanical parts adapted to the electrical Mini-Baja used on the essays for this specific research. The structure was mounted in aluminum, and the transmission is powered by belt and pulleys directly connected to the motor in a 5:1 ratio.

In spite of the much greater efficiency of electrical motors in relation to internal combustion motors, EVs still need drastic reductions in aerodynamic drag and in rolling resistance, in order to increase their range. This relies on a new design for the tires and vehicle shape. Aerodynamic drag, the force that opposes movement, is increased by the quadratic power of the velocity, and can be reduced in two different ways. First, the overall speed of the vehicle can be reduced, but this makes the vehicle less attractive to consumers. Second, by diminishing the aerodynamic drag coefficient that today varies from 0.3 to 0.4. Special graphic designs for the EV can deliver a 0.2 coefficient value. Another reduction can be achieved by using more rigid and narrower tires, although comfort could be adversely affected. Doubling pressure for common tires, the 0.01 to 0.02 average range for the rolling resistance can be lowered to the 0.004 to 0.007 range (Scaduto and Fenton, 1993). An intelligent method to increase EV efficiency is through the use of regenerative braking, instead of common friction brakes that remain on the vehicle for occasions in which a very fast stop is demanded.

This paperwork discusses the implementation of a low-cost, open-loop PWM inverter using a three-phase induction motor, specifically built for the mini-baja EV. The option for the development of an EV equipped with a three-phase induction motor is based on the ease of implementation of speed drive, no start-up circuit, and easiness of movement reversion.

3. The Speed Control

Induction motors are essentially constant speed motors, if connected to constant voltage and frequency source. The operation speed for induction motor is directly related to the synchronous speed. If load torque increases, the drop in speed will be very small, which is convenient for constant speed applications.

Currently, the main speed control techniques for three-phase induction motors are vector control, which employs digital signal processors, and PWM (Anonymous, 1994; Rashid, 1993). By far, the open-loop PWM is the easiest technique to implement, if motor speed does not need to be very accurate, as is the case on EVs, where the driver controls the speed through the accelerator pedal.

3.1. The Constant Flux Control Method

The output torque of a three-phase induction motor, M_d, can be calculated through (1), where P is the number of poles, V_m is the counter electromotive force (CEMF), w_s is the angular frequency of the stator current, w_r is the angular frequency of the rotor current, R_r is the rotor resistance, and L_{lr} is the locked rotor inductance (Anonymous, 1994; Fitzgerald *et allii*, 1992).

$$M_d = 3\ (P/2)\ (V_m/w_s)^2\ [w_r/R_r^{\ 2} + (w_r\ L_{lr})^2]\ R_r. \tag{1}$$

Equation (1) implies that the output torque of the machine will depend only on w_r, irrespective of the stator frequency, w_s, provided the ratio V_m/w_s is kept constant. This ratio is the peak amplitude of the airgap flux, ψ_m:

$$\psi_m = V_m/w_s. \tag{2}$$

By maintaining airgap flux constant, and varying the stator frequency w_s, a family of torque versus speed curves can be achieved for the motor, as shown in figure 1. This method of speed control is known as constant flux control (Anonymous, 1994).

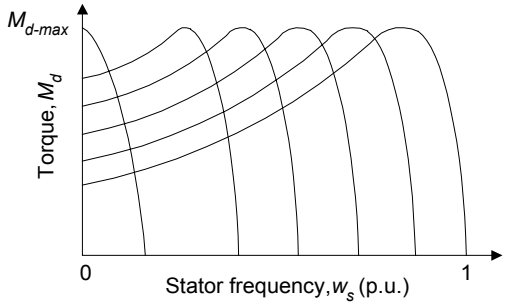

Figure 1. Constant-flux torque versus frequency curves.

Figure 1 implies that this technique can meet any load torque, within the capability of the motor, at all speeds, up to the rated speed. Furthermore, it is possible to obtain high torque for starting the motor, by operating it at a low frequency.

Nevertheless, the implementation of the above method is not straightforward, as the CEMF cannot be measured directly. And although it can be calculated by measuring the motor terminal voltages and currents, this implies on increasing control circuit complexity and cost (sensors, conditioning circuits, analog to digital converters, DSPs, etc). It must be taken into account that a seemingly small cost increase in a car component (as for example, in the integrated circuit utilized in the control circuitry) leads to considerable income lost, in serial production of the car. Fortunately, for practical purposes, the above technique can be implemented in an approximate manner, by keeping the V_s/w_s ratio constant, as the stator terminal voltage, V_s, and the CEMF are reasonably close in magnitude at almost all, but at low speeds. At low speeds, keeping V_s/w_s constant is not equivalent to keep the flux constant, resulting in a much lower torque. In this work, the torque decrease at low speed has been overcome by giving a boost on stator voltage, V_s, above the constant V_s/w_s, as shown in figure 2.

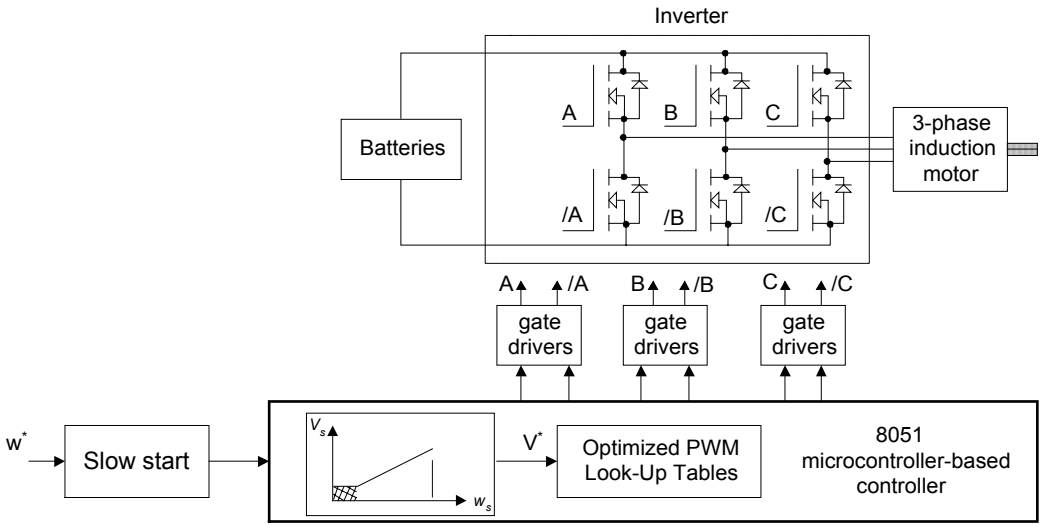

Figure 2. Block diagram for the controller.

3.2. Pulse Width Modulation Purpose and Inverter

Adjustable speed drives have undergone great structural modifications. At first, their working principle was analogical, but nowadays it has become digital, thanks to the astonishing technological advance on solid-state power switches and microprocessors. The speed drive can be divided into two parts: the inverter (or dc-ac converter) and PWM circuit. A battery feeds the inverter, which is gated by the PWM circuit, in order to feed the three-phase induction motor, in accordance with the commanded speed, w^*, as illustrated in figure 2.

The basic purpose of the PWM method is to produce the required amplitude and frequency of the fundamental, while moving the energy in the harmonics to a higher range in the frequency spectrum. At such high frequencies, the motor inductance will exhibit substantial reactance, therefore limiting the harmonic currents drawn from the inverter and reducing the resulting torque pulsations created by these high-frequency harmonics. The inertia of the mechanical system also helps filtering out high frequency torque pulsations, allowing the motor to run smoothly.

3.3. Digital Project Difficulties

Sinusoidal current generation by using PWM and inductive loads is commonplace. However, its digital implementation with a low-cost microcontroller is not straightforward, mainly if it is to drive a three-phase induction motor in a wide speed range, and yet maintaining constant torque, as is the case with the EV.

In a battery-fed inverter, with a triangular carrier wave and sinusoidal modulating signal, the modulation index must be varied, in order to keep the flux constant (and so the motor's output torque), whereas different speeds are imposed to the motor. Furthermore, a high frequency carrier, say 1.5 kHz, is needed to ease filtering of high-frequency current harmonics. Also, harmonic content can be reduced by using a carrier wave whose frequency is much higher than the modulating signal frequency (Rashid, 1993). In a microcontroller-based implementation, however, this has two important implications: 1) The software must compare the two waves a great number of times in every carrier period, in order to generate the PWM signal. Moreover, for a three-phase inverter, the computational load becomes three times

greater. 2) To detect the exact instant where the triangular carrier wave crosses the three reference sinusoids, the system's sampling frequency must be high enough.

For the sake of illustration, a 30-kHz sampling frequency (that would result in modest 20 samples per cycle of a 1.5-kHz carrier wave), would leave the microcontroller only 33.3 μs between samples to do all the job (typically branching to timer interrupt service routine, comparing the triangular carrier wave with the three sinusoidal references, carrying out conditional jumps, updating the three PWM control signals, and returning from interrupt, besides reading the speed reference signal and calculating the suitable modulation index). On-line computed switching instants could be a much difficult, if not impossible, task to a low-cost 8-bit microcontroller.

Pre-calculated PWM control signals burned as tables into the microcontroller´s Read Only Memory (ROM) can be an appealing solution, since it avoids much of the computational load already mentioned (Simard *et alli*, 1991). Nevertheless, as in the EV application frequency as low as 5 Hz must be generated, an unreal amount of ROM would be required to save PWM control signals of, say, a dozen different frequencies. Using a 30-kHz sampling frequency, PWM control signals for a cycle of the 5-Hz modulating signal would alone occupy 6,000 ROM locations, whereas the same PWM signals for a 60-Hz modulating sinusoid would occupy only 500 ROM positions. In this work, a technique has been employed which besides solving the problem of the size of the tables, for low frequencies, synchronizes the modulation, avoiding pulsating torques and low frequency harmonics.

3.4. Optimization of PWM Tables

In this work, a simple technique has been devised to reduce the PWM tables' size to be burned into the microcontroller's ROM, which decreases the need for a fast microcontroller as well as for large ROM size, making it possible to use standard industry-proven, low-cost 8-bit microcontroller as the central control block of an experimental-EV PWM drive (Marcelino and Fiorotto, 1997).

A first step to generate a PWM table for a given modulating sinusoid consists on choosing a carrier wave whose frequency is an exact multiple of the modulating signal. Furthermore, the triangle carrier is forced to have a fixed number of cycles within one modulating cycle, no matter the modulating frequency, so that the number of pulses in each cycle of the PWM output voltage is fixed (and does not depend on the output frequency). In other words, the resulting table size for a particular output frequency depends only on the sampling frequency. The criteria to select the number of pulses and the sampling frequency will be discussed in the next subsection.

Table 1 illustrates the working principle of the optimization technique. The left hand column contains the first 18 non-optimized samples for fictitious three-phase PWM control signals, whereas the right hand column contains the 12 optimized samples for the same PWM signals. As Table 1 shows, reduction in table (column) size is obtained by saving the samples (bytes) representing the desired PWM signals and their repetition numbers. Therefore, the greater the samples' repetition times, the shorter the optimized chart.

Table 1. Normal and Optimized Speed Charts (sample number reduction: 18 to 12)

NORMAL TABLE	OPTIMIZED TABLE
A	A
a	4
a	b
a	3
b	a
b	2
b	c
a	5
a	a
c	1
c	c
c	3
c	
c	
a	
c	
c	
c	

a,b,c: distinct byte values

3.5. Practical Considerations

The ratio, n, between the frequency of the triangle carrier, f_c, and the frequency of the modulating sinusoids, f_m, must fulfill the criteria summarized bellow (Anonymous, 1994).
1) n must be an integer number, in order to synchronize triangle carrier and modulating sinusoids, so that the output voltage is periodic and free from sub-harmonics.
2) n must be multiple of 3, to ensure that the output voltage waveforms produced by each inverter phase is the same.
3) n must be an odd number, in order to get the output voltage rid of even harmonics.
4) n must be the greatest possible number, to ease high-frequency harmonics filtering by motor's inductance.
5) n must be the smallest possible number, so that the requirement for a fast-response PWM control circuit are loose.
In this work, the chosen value for n was 21 for it fulfilled all of these recommendations.
On PWM table calculations, which have been done by a program written in C language, by choosing a sampling frequency which is a multiple of four of the triangle carrier's frequency eases synchronization of the carrier with the three sinusoidal references. For a desired output frequency, f_s, the number of samples, N, per carrier period is calculated through (3):

$$N = 1 / (f_s \, n \, t_s) \tag{3}$$

where t_s is the sampling period, i.e., the interval between two consecutive samples of the PWM signals saved on ROM. The sampling period is also the critical time the microcontroller has to carry out all tasks and, for the Intel 80C31microcontroller employed in this work, this time interval is circa 22 μs, for a crystal oscillator of 12 MHz.

Therefore, for f_s = 60 Hz, by means of (3), one gets N = 36.075. As the result must be a integer and multiple of four, N is approximated to 36 and, using (3) again, the real stator frequency is 60.125 Hz. The small deviation between the desired and the actual stator frequency is no problem for the EV application.

To generate a 60-Hz stator frequency, the number of PWM samples in the ROM table is 756 (i.e., n x N = 21 x 36). In this work, PWM tables have been created for twelve distinct stator frequencies, from 5 Hz to 60 Hz, every 5 Hz. In each frequency, a suitable sampling frequency has been employed, in order to keep the number of PWM samples in ROM equal to 756. The sampling periods, for some of the frequencies, have resulted in a real, but not integer, numbers. However, as the microcontroller must be interrupted in integer intervals of microseconds (a 12 MHz crystal oscillator has been used), in those cases, the required stator frequencies have suffered small adjustments (e.g., 55.114 Hz in lieu of 55 Hz), all of them negligible from the practical point of view. To the so generated PWM tables has been applied the table reduction technique already described, before burning the samples into ROM.

The optimization and the synchronization techniques have allowed that the table for 5 Hz, initially occupying 6000 ROM locations, could occupy only 756 ROM locations, resulting in a sampling frequency around 4000 Hz. Although this frequency is inside of the audio range, the noise is minimum since the amplitude is well reduced by the constant V/f requirement.

4. Vehicle Test and Results

For the Mini-Baja EV prototype, motor manufacturer "EBERLE do Brasil" has adapted a squirrel-cage three-phase induction motor, which has 2 poles and 1120 W rated power at 110 V and 60 Hz.

During the tests, the EV has been fed through a 100-V mains rectified dc-power supply, in lieu of batteries. An extension cord has been employed that allows the vehicle to go around. The maximum speed obtained in the assays has been 18 km/h. Controlled acceleration and regenerative breaking has been employed. The inverter circuitry includes 6 N-channel power MOSTETs (IRF450 Insulated-Gate Bipolar Transistors) and their gate drives (IR2110), all manufactured by International Rectifier Inc..

4.1. Measurements of Motor Current

Electric current measurements have been effected in one of the machine's phase, by using a 160 mΩ resistor as current sensor and connecting it in series with the phase winding. Current waveforms have been recorded through a handheld digital oscilloscope. Figure 3 shows the phase current following a step change, from 0 to 60 Hz, in the frequency reference, which corresponds to the phase current due to a speed step requirement. In this essay, the recording time (circa 250 ms) has been chosen to focus the excessive phase current resulting from the sudden frequency change, which ultimately is caused by the high rotor slip level during motor start up. Using a suitable scanning speed, the almost sinusoidal nature of the current waveform has been observed. Figure 4 shows the phase current waveform for the same change in frequency requirement (0 to 60 Hz) as in the last case. This time, however, the control algorithm limits the motor's acceleration, imposing four intermediate frequencies to the inverter's output voltage. This results in a lower slip of the rotor and thus in smaller transient currents. From the EV driver's viewpoint, however, the acceleration sensation is normal, because each intermediate frequency lasts only 150 ms. Nevertheless, limiting current transients,

besides lowering solid-state switches (IGBTs) specification (which have to withstand smaller currents), lessen stator-coils' Joule effect loss (proportional to current square power), which ultimately extends the EV's battery life. In addition, unlike most "soft starters" figure 4 shows that frequency transitions during accelerations are carried out during zero voltage crossing. This diminishes harmonics and sub-harmonics generation.

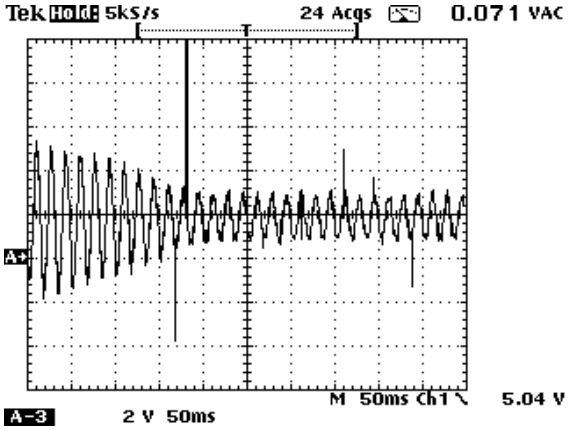

Figure 3. Phase current following a sudden change of speed.

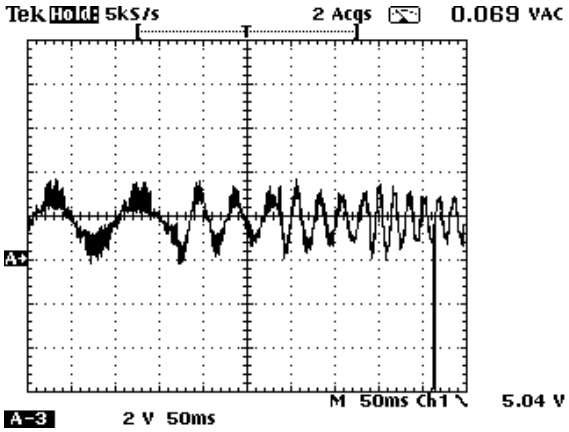

Figure 4. Phase current following a controlled change of speed.

5. Conclusion

Whereas mass production and worldwide sales of electric cars depend on lowering battery prices and increased battery autonomy, today's EVs are undoubtedly suitable at least as the family's second vehicle and this could help to improve air quality in big cities, through the reduction in carbon dioxide emissions, and world's dependence on fossil fuel.

In this paperwork, a simple technique to generate three-phase PWM control signals with low-cost 8-bit microcontroller has been presented that allowed the realization of a constant-torque variable speed drive for a three-phase induction motor. The motor, inverter and controller have been tailored to a modified mini-Baja type EV, in which the essays have shown that the speed control algorithm can significantly reduce the transient current amplitudes, thus increasing battery life and allowing the use of cheaper semiconductor switches.

6. References

Anonymous, S., 1994, "A Tutorial in AC Induction and Permanent Magnet Synchronous Motors", Analog Devices Inc., Massachusetts, pp. 25–31.

Cooper, A., 2005, "Develoment of a High-Performance Lead-Acid for Battery for New-Generation Vehides", Journal of Power Sources (June) 144 (2): pp. 385-394.

Cocconi, A. & T. Gage, 2002, "A plug for Plug-in Cars", *IEEE Spectrum* (April) 2002, pp. 14-15.

Faiz J, Moayed-Zadeh K , 2005, "Design of Switdhed Reluctance Machine for Starter;Generator of Hybrid Electric Vehicle", Electric Power Systems Research (August) 75 (2-3): pp. 153-160.

Fitzgerald, A. E., Kingsley Jr, C., and Umans, S. D., 1992, "Electric Machinery", McGraw-Hill, New York.
Lam, L.T., Haigh, N.P., Phyland, C.G., 2005, "Novel Technique to Ensure Battery Reliability in 42-V PowerNets for New-Generation Automobiles", Journal of Power Sources (June) 144 (2): pp. 552-559.
Marcelino, M. A. and Fiorotto, F.A., 1997, "Discrete, optimized and synchronous PWM generation", Brazilian Patent PI97040810-9 (in Portuguese).
Naunim, D., 1996, "Electric Vehicles", *Proc. IEEE International Symposium on Industrial Electronics*, Vol. 1, pp.11-24.
Rashid, M. H., 1993, "Power Electronics–Circuits, Devices, and Applications (2nd ed.)", Prentice Hall, Upper Saddle River.
Riezenman, M. J., 1998, "EVs: The Road Ahead", *IEEE Spectrum* (December), pp. 42-51.
Scaduto, T.and Fenton, B.C. , 1993, "The EV Revolution. Popular Electronics", Vol. 10, no 4 (April), pp. 31-36.
Simard, R., A., Cheriti, T. A., Meynard, K. Al-Haddad, and Rajagopalan, V., 1991, "A Eprom-based PWM Modulator for a Three-phase Soft Commutated Inverter", IEEE Transactions on Industrial Electronics, Vol. 38, No. 1, pp.79-81.

6. Responsibility notice

The authors are the only responsible for the printed material included in this paper.